Calculating van der Waals-London dispersion spectra and Hamaker coefficients of carbon nanotubes in water from *ab initio* optical properties

R. F. Rajter
Department of Materials Science, Massachusetts Institute of Technology, Cambridge, Massachusetts 02139

R. H. French
DuPont Company Central Research, Wilmington, Delaware 19880-0400

W. Y. Ching
Department of Physics, University of Missouri—Kansas City, Kansas City, Missouri 64110-2499

W. C. Carter and Y. M. Chiang
Department of Materials Science, Massachusetts Institute of Technology, Cambridge, Massachusetts 02139

The van der Waals-London dispersion (vdW-Ld) spectra are calculated for the $[9,3,m]$ metallic and $[6,5,s]$ semiconducting single wall carbon nanotubes (SWCNTs), graphite, and graphene (a single carbon sheet of the graphite structure) using uniaxial optical properties determined from *ab initio* band structure calculations. The $[9,3,m]$, exhibiting metallic optical properties in the axial direction versus semiconducting optical properties in the radial direction, highlights the strong anisotropic nature of metallic SWCNTs. Availability of both efficient *ab initio* local density band structure codes and sufficient computational power has allowed us to calculate the imaginary parts of the frequency dependent dielectric spectra, which are then easily converted to the required vdW-Ld spectra for Hamaker coefficient calculations. The resulting Hamaker coefficients, calculated from the Lifshitz quantum electrodynamic theory, show that neither graphite nor graphene are accurate model materials for estimating the Hamaker coefficients of SWCNTs. Additionally, Hamaker coefficients were calculated between pure radial-radial, radial-axial, and axial-axial components of both SWCNTs. Analysis of these coefficients reveals that the vdW-Ld interactions will depend on both chirality and the particular orientation between neighboring SWCNTs. The minimization of energy, with respect to orientation, predicts that vdW-Ld alignment forces will arise as a result of the anisotropic optical properties of SWCNTs. © *2007 American Institute of Physics.*
[DOI: 10.1063/1.2709576]

I. INTRODUCTION

The properties of single wall carbon nanotubes (SWCNTs) have been extensively documented[1–5] and their structures hold much promise for optical, electronic, and structural applications. Because incremental changes in the SWCNT chirality, $[n,m,*]$,[1,2] are known to produce nonincremental effects in the electronic band structure, interactions between SWCNT types (metallic and semiconducting)[6] and specific chiralities are significant.[7] Exploitation of these properties depends on the processing methods to incorporate SWCNTs into devices; and success with these processing methods depends on our ability to quantitatively determine, predict, and control intermolecular forces. The van der Waals-London dispersion (vdW-Ld) interactions and forces,[8,9] being both long range and universal, are of critical importance and have two contributions to their anisotropy[10,11]: The first source arises from the anisotropy of the electronic structure and the interband transitions of the optical properties of the materials; the second arises from the morphology of each component in the system (e.g., the cylindrical nature of nanotubes).[12]

In this work we have calculated the electronic structure and optical properties of graphite, graphene, and the $[6,5,s]$ and $[9,3,m]$ SWCNTs. The calculated uniaxial optical prop-erties are then used to determine the vdW-Ld spectra, which are the critical inputs to enable a quantitative determination of the Hamaker coefficients for the vdW-Ld interaction energy formulation.[13] We then calculate these full spectral Hamaker coefficients for graphite, graphene, and the individual SWCNT chirality components interacting with each other (i.e., radial-radial, radial-axial, and axial-axial) across a water medium. The optical anisotropy gives rise to anisotropic vdW-Ld dispersion energies,[14,15] which can result in torques promoting configurational order in aqueous suspensions.

II. METHODS

The anisotropic (uniaxial) optical properties and vdW-Ld spectra for the $[9,3,m]$, $[6,5,s]$, graphite, and graphene have been calculated for interband transition energies up to 45 eV. This was done using an *ab initio* orthogonalized linear combination of atomic orbitals (OLCAO)–density functional theory (DFT) technique[16] followed by full dipole matrix element calculations to determine the imaginary part of the frequency dependent dielectric functions,[17–20] Im[ε], of the SWCNTs in both primary directions (axial and radial). The calculated dielectric functions are shown in Fig. 1. Mintmire and White[21] also reported the dielectric function of a $[7,5,s]$
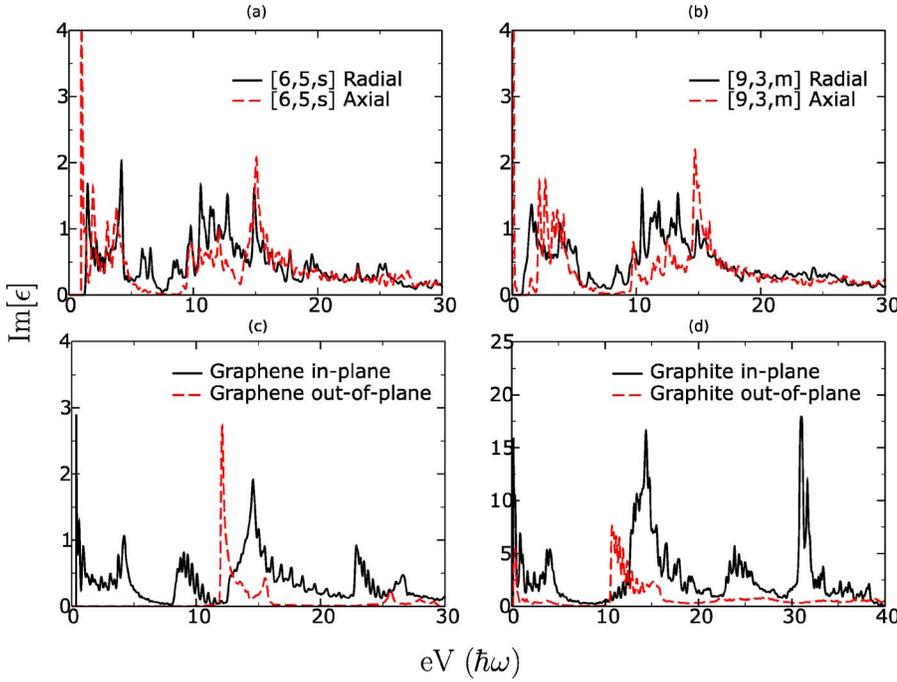
FIG. 1. *Ab initio* Im$[\varepsilon](\omega)$ spectra data of (a) $[9,3,m]$, (b) $[6,5,s]$, (c) graphene, and (d) graphite in all unique directions. The $[9,3,m]$ has metallic features in the axial direction as can be seen by the large impulse that has a maximum of 255 at 0.03 eV. Graphene's in-plane spectra is in agreement with some of the general features of the SWCNTs spectra, but not all of them. Graphene's out-of-plane spectra is completely different. Graphite's Im$[\varepsilon](\omega)$ spectra are considerably larger than the SWCNT.

semiconducting SWCNT with results comparable to ours.

Once the Im$[\varepsilon]$ spectra have been calculated up to 45 eV, the vdW-Ld spectra, $\varepsilon(\iota\xi)$, are obtained via the Kramers-Kronig (KK) transform[8,13]

$$\varepsilon(\iota\xi_n) = 1 + \frac{2}{\pi}\int \frac{\omega\,\text{Im}[\varepsilon](\omega)}{\omega^2 + \xi^2}d\omega. \quad (1)$$

Because experimental and *ab initio* data are often finite, analytical wings of the form $e^{-\beta*\omega}$ are often attached in order to effectively approximate data beyond the upper cutoff energy limit.[13] This wing approximation gives sensible results as long as there are no large contributions occurring beyond the selected cutoff energy. We attached a high energy wing attachment at 40 eV because our calculated Im$[\varepsilon(\omega)]$ spectrum for the graphite's in-plane direction has a considerably large Im$[\varepsilon]$ contribution around 32 eV and additional contributions in the 34–38 eV range. The $[9,3,m]$ and $[6,5,s]$ SWCNTs essentially have no contributions in the 30–40 eV range, so any cutoff between 30 and 40 eV yields vdW-Ld curves that differ by less than 0.2% in magnitude.

For our water vdW-Ld spectrum, we used the index of refraction matching oscillator model as given by Parsegian.[8] The various water models available in the literature can fluctuate in $\varepsilon(\iota\xi)$ by as much as 0.2 along much of the UV frequency range. This variation can dramatically effect the outcome of a quantitative or qualitative analysis of the resulting Hamaker coefficients and vdW-Ld energies.[22] The Parsegian water spectrum agrees very well with the spectrum given by Ackler *et al.*[23] in the UV range, has the proper index of refraction in the visible range, and includes the proper and very important zero-frequency term behavior.

The full spectral Hamaker coefficient (A_{LmR}) of the vdW-Ld interaction energy for two macroscopic bodies dispersed in a medium is typically written as

$$G = C(\text{geometry}) * D(\text{LD spectra}) \approx -\frac{g}{p(d)} * A_{LmR}, \quad (2)$$

where g is a collection of geometric/morphology factors that depends upon on the shapes of bodies in the system and $p(d)$ is a generalized distance scale factor[24] (typically of the form d^n, where n is a constant between 1 and 6). A_{LmR} is the Hamaker constant, which depends *only* on the vdW-Ld spectra of the components when in the two semi-infinite half-space arrangement.[13] The L and R subscripts denote the arrangement of the interacting materials as the left and right half-spaces while m represents the intervening medium between L and R.

When retardation effects are taken into consideration, A_{LmR} is typically referred to as the Hamaker "coefficient" because it is now a function of the separation distance between the half-spaces.[25] This can lead to Hamaker coefficients that behave in complex ways (e.g., it can switch sign and/or increase in magnitude as a function of the separation distance) when the system has at least three unique vdW-Ld spectra and at least two of them cross. We utilize the full Lifshitz summation to calculate A_{LmR} as a function of distance d in the following form:[26]

$$A_{LmR}(d) = \frac{3}{2}kT\sum_{n=0}^{\infty}{}'\int_{r_n}^{\infty} x\ln[(1-\Delta_{Lm}\Delta_{Rm}e^{-x})$$
$$\times(1-\overline{\Delta}_{Lm}\overline{\Delta}_{Rm}e^{-x})]dx, \quad (3)$$

$$\Delta_{ij} = \frac{x_j\varepsilon_i - x_i\varepsilon_j}{x_j\varepsilon_i + x_i\varepsilon_j}, \quad \overline{\Delta}_{ij} = \frac{x_j\mu_i - x_i\mu_j}{x_j\mu_i + x_i\mu_j}, \quad (4)$$

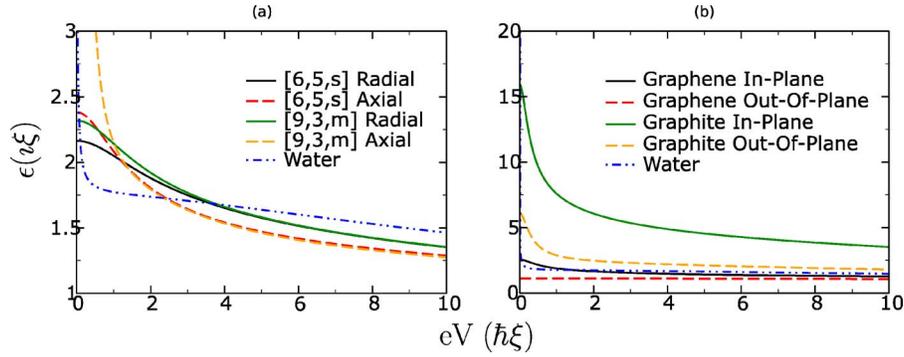$$x_i^2 = x^2 + \left(\frac{2d\xi_n}{c}\right)^2(\varepsilon_i\mu_i - \varepsilon_m\mu_m), \quad (5)$$

FIG. 2. The $\varepsilon(\iota\xi)$ directional vdW-Ld spectra of (a) $[9,3,m]$ and $[6,5,s]$, (b) graphene and graphite for each material's distinct, optically independent directions. The Parsegian water oscillator spectra is included in each graph for comparison, and rises to 78.8 at 0 eV. The $[9,3,m]$ axial direction in (a) peaks with a value of 92 at 0 eV, while graphite's axial and radial components in (b) max out at 15.9 and 6.1, respectively. Whenever vdW-Ld spectra cross, there is a potential for the contributions in the Eq. (3) summation to switch sign. This is the source of interesting phenomenon, such as the vdW-Ld controlled equilibrium wetting thicknesses of water on ice (Ref. 30).

$$r_n = (2d\varepsilon_m^{1/2}\mu_m^{1/2}/c)\xi_n. \tag{6}$$

The prime in the summation denotes that the $n=0$ term is multiplied by a half. It should be noted that not all frequencies contribute to the dispersion interaction. The Lifshitz sum is over discrete frequencies, $\xi_n=2\pi kTn/\hbar$ for $n=1,2,\ldots,\infty$ and, therefore, includes interband transitions at large energies. All ε are a function of these discrete frequencies. Our CNTs are nonmagnetic, so all μ terms contribute nothing to the overall summation, but are left in for completeness.

For our graphite and graphene calculations, we used a uniaxial formulation for two half-spaces interacting across an isotropic medium in order to properly capture the interactions arising from both the in-plane and out-of-plane optical properties. The full form is only slightly more complicated than the isotropic formulation in Eq. (3) and it takes into account the spectra of both the radial and axial directions simultaneously. In the limit of very small separation (i.e., near contact), the formula for two uniaxial half-spaces, having their principle axes aligned perpendicular to the interface, can be simplified to[8]

$$A_{LmR} = \frac{3\kappa T}{2}\sum_{n=0}^{\infty}\sum_{j=1}^{\infty}\frac{(\overline{\Delta}_{Lm}*\overline{\Delta}_{Rm})^j}{j^3}, \tag{7}$$

$$\overline{\Delta}_{Lm} = \frac{\sqrt{\varepsilon_{L\perp}*\varepsilon_L}-\varepsilon_m}{\sqrt{\varepsilon_{L\perp}*\varepsilon_L}+\varepsilon_m}, \quad \overline{\Delta}_{Rm} = \frac{\sqrt{\varepsilon_{R\perp}*\varepsilon_R}-\varepsilon_m}{\sqrt{\varepsilon_{R\perp}*\varepsilon_R}+\varepsilon_m}. \tag{8}$$

For graphite and graphene, the parallel direction, $\parallel$, is the in-plane direction of the honeycomb sp^2 lattice while the perpendicular direction, $\perp$, is aligned with the principle axis normal to the honeycomb sp^2 lattice.

III. RESULTS

Figure 1 shows the *ab initio* dielectric function, $\text{Im}[\varepsilon(\omega)]$, for the $[9,3,m]$ metallic and $[6,5,s]$ semiconducting tubes' radial and axial components. The dielectric functions for graphite and graphene are included for comparison. The differences that exist between all of these spectra are a result of each materials electronic band structure properties, which themselves are determined by stacking, curvature, and chirality effects. It is interesting to note that

for the metallic $[9,3,m]$ SWCNT, only the axial direction exhibits the typical Drude metal behavior[27] as exhibited by the Lorentz oscillator peak of transitions centered at 0 eV. This metallic SWCNT exhibits semiconducting features in the radial direction, with a band gap and no significant interband transitions visible in the dielectric function below 0.8 eV. This demonstrates the strong uniaxial nature of the electronic structure and optical properties of nominally metallic SWCNTs. The semiconducting $[6,5,s]$ SWCNT has semiconducting features in both the axial and radial directions and this produces less vdW-Ld interaction anisotropy, although variations are still present.

Figure 2 compares directional vdW-Ld spectra of the $[9,3,m]$ and $[6,5,s]$ SWCNTs against graphite, graphene, and water. Although graphene's in plane spectra appears to be similar in nature to three of the CNT spectra, the differences are substantial enough to deem it unsuitable for all but the crudest of approximation purposes. The differences in these spectra may be enough to change the Hamaker coefficient's sign and magnitude in a given multilayered and multicomponent system. Under no circumstances should graphite's spectra be used, as it is completely different from that of any CNT. The $[9,3,m]$'s axial vdW-Ld has a low frequency spike similar to that of graphite at 0 eV, but that is where the similarities end. Therefore, neither graphite or graphene can be used to even crudely approximate the vdW-Ld spectra of the $[9,3,m]$'s axial direction.

Having acquired the vdW-Ld spectra, we then calculated the room-temperature, full-spectral Hamaker coefficient for various configurations of graphite, graphene, and the $[9,3,m]$ and $[6,5,s]$ SWCNTs in a water medium. Graphite has previously received attention primarily as a colloidal particle in solution. In the problem of interest to Dagastine *et al.*,[28] dispersion in carbon black suspensions, they take a similar approach to ours, considering the uniaxial optical properties of graphite and representing the carbon black as semi-infinite half-spaces to determine the Hamaker constant appropriate for close separations. Using Eq. (7), our calculations of 223 and 97 zJ for the graphite-vacuum-graphite and graphite-water-graphite systems compares very favorably to the values of 253 and 115 zJ calculated by Dagastine *et al.*
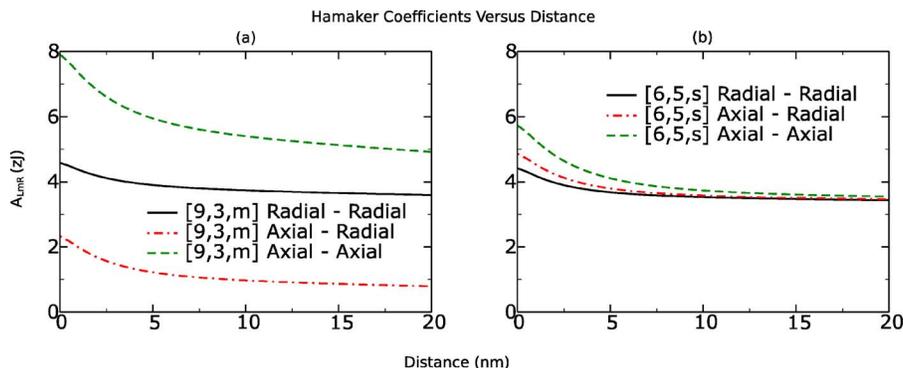
FIG. 3. The Hamaker coefficients for all axial-axial, axial-radial, and radial-radial interactions of the (a) $[9,3,m]$ and (b) $[6,5,s]$ SWCNTs. For the $[9,3,m]$, the weakest interaction is the axial-radial interaction, which is a consequence of the elimination of an otherwise large attractive term at the zero frequency interaction. The differences in the Hamaker coefficients for the $[6,5,s]$ component interactions are much more subtle in comparison to the $[9,3,m]$ because its anisotropy is there but not nearly as strong.

The 15% difference in our calculations suggests that there is a small discrepancy in the magnitudes of our vdW-Ld spectra.

Graphene's calculated Hamaker coefficients are much smaller than the values calculated for graphite, which is just what one would expect considering the large difference in the magnitudes of the vdW-Ld spectra curves in Fig. 2. Using the same method employed in the graphite calculation, we calculated gaphene-vacuum-graphene and graphene-water-graphene at 9 and 13 zJ, respectively. Not only are these values an order of magnitude lower than the values for the graphite system, but the attraction of graphene to itself actually increases when moved from a vacuum to a water medium.

For the SWCNTs, we are primarily interested in analyzing the vdW-Ld energy anisotropy arising from the material properties of the system rather than the geometrical considerations [see Eq. (2)]. By returning to the simple half-space formulation of Eq. (3) and focusing on the Hamaker coefficient, we are able to analyze the interaction strengths and retardation effects versus distance between each set of uniaxial components (radial-radial, radial-axial, and axial-axial) across a water medium. To do this, we use one pure radial or pure axial component from the particular SWCNT and convert it into a isotropic half-space of that component. This analysis gives us the ability to determine which particular components of the vdW-Ld interaction are the strongest and if the differences are large enough to drive alignment. The authors wish to stress that this simple analysis results in qualitative relationships because the geometric considerations of all components of the system will, in fact, be coupled with a material's optical anisotropy and could effect the magnitude of these interactions. Formulations for interactions between anisotropic cylinders are under development.

Figure 3 shows the room-temperature, full-spectral Hamaker coefficients of the SWCNT axial-axial, axial-radial, and radial-radial component interactions in water. It is clear that previously calculated A_{LmR} values of graphite in water (110 zJ) are much too large to be used in describing SWCNT vdW-Ld interactions. A_{LmR} energies for graphene tend to be closer in magnitude with the SWCNTs, but this is more of a result of our choice of water as the medium between them. If we changed the medium from water to air or an organic solvent, the magnitudes would not necessarily change by the same amount or even in the same direction. For example, if the intervening medium is changed from water to vacuum, the radial-radial and axial-axial Hamaker constant calculations for the $[9,3,m]$ rise from values around 6–8 zJ to values around 33–35 zJ while graphene goes drops from 13 zJ down to 9 zJ.

Figure 3 also demonstrates how changes in the vdW-Ld spectra (Fig. 2) can lead to a rich set of results based on the multicomponent interaction.[29] The $[9,3,m]$ axial and radial vdW-Ld spectra between 2.4 and 3.8 eV and at 0 eV reside on opposite sides of the water spectra, which results in Eq. (4) adding repulsive contributions into the otherwise attractive summation. The stacking arrangement at and near the zero frequency term is the primary reason why the $[9,3,m]$ axial-radial Hamaker coefficient is noticeably weaker in energy than both the axial-axial and radial-radial terms. Therefore, a geometrical arrangement that maximizes the axial-axial and radial-radial interactions will be the most energetically favorable, leading to vdW-Ld torques to achieve this alignment.

A similar analysis can be done for the $[6,5,s]$, although the effect is more noticeable for a $[9,3,m]$ of a given length of SWCNT. However, since the total vdW-Ld energy can be increased by scaling up the length, a longer $[6,5,s]$ could conceivably have a larger alignment force than a shorter $[9,3,m]$.

There are many other avenues to begin exploring, such as the effects of other chiralities, the interactions with substrates of varying material properties, and the role of surfactant coatings upon the SWCNTs. Now that we actually have the data available, we can begin to search through these other areas with the eventual goal of being able to design systems to exploit the differences in these interactions with respect to orientation and chirality.

IV. CONCLUSIONS

Quantitative, full spectral, room temperature, Hamaker coefficients based on *ab initio* optical properties and vdW-Ld

spectra show that the vdW-Ld interactions for SWCNTs depend strongly on the optical anisotropy arising from the chirality $[n,m,*]$. Additionally, the vdW-Ld spectra for both SWCNT types (metallic and semiconducting) cannot be approximated by graphite or graphene because the resulting Hamaker coefficient calculations are either a magnitude too large (graphite) or they do not follow the proper trend behavior when switching from one medium to the next (graphene). Simple calculations of the different radial and axial component interactions predict a vdW-Ld alignment force, which could be potentially useful for various enrichment and/or assembly processes.

ACKNOWLEDGMENTS

[1] C. T. White and J. W. Mintmire, J. Phys. Chem. B **109**, 52 (2005).
[2] V. N. Popov, Mater. Sci. Eng., R. **43**, 61 (2004).
[3] Ge. G. Samsonidze, R. Saito, N. Kobayashi, A. Gruneis, J. Jiang, A. Jorio, S. G. Chou, G. Dresselhaus, and M. S. Dresselhaus, Appl. Phys. Lett. **85**, 5703 (2004).
[4] M. S. Dresselhaus, G. Dresselhaus, R. Saito, and A. Jorio, Phys. Rep. **409**, 47 (2005).
[5] M. S. Dresselhaus and P. C. Eklund, Adv. Phys. **49**, 705 (2000).
[6] I. Cabria, J. W. Mintmire, and C. T. White, Phys. Rev. B **67**, 121406 (2003).
[7] M. Zheng, A. Jagota, E. D. Semke, B. A. Diner, R. S. McLean, S. R. Lustig, R. E. Richardson, and N. G. Tassi, Nat. Mater. **2**, 338 (2003).
[8] V. A. Parsegian, *Van der Waals Forces* (Cambridge University Press, Cambridge, MA, 2005).
[9] E. M. Lifshitz, Sov. Phys. JETP **2**, 73 (1956).
[10] B. W. Ninham and V. A. Parsegian, J. Chem. Phys. **52**, 4578 (1970).
[11] R. Podgornik and V. A. Parsegian, Phys. Rev. Lett. **80**, 1560 (1998).
[12] R. F. Rajter, R. Podgornik, V. A. Parsegian, R. H. French, and W. Y. Ching (submitted).
[13] R. H. French, J. Am. Ceram. Soc. **83**, 2117 (2000).
[14] K. M. Knowles, J. Ceram. Proc. Res. **6**, 10 (2005).
[15] K. M. Knowles and S. Turan, Ultramicroscopy **83**, 245 (2000).
[16] W. Y. Ching, M. Z. Huang, Y. N. Xu, W. G. Harter, and F. T. Chan, Phys. Rev. Lett. **67**, 2045 (1991).
[17] R. H. French, S. J. Glass, F. S. Ohuchi, Y. N. Xu, and W. Y. Ching, Phys. Rev. B **49**, 5133 (1994).
[18] W. Y. Ching, Y. N. Xu, and R. H. French, Phys. Rev. B **54**, 13546 (1996).
[19] Y. N. Xu, W. Y. Ching, and R. H. French, Phys. Rev. B **48**, 17695 (1993).
[20] Y. N. Xu and W. Y. Ching, Phys. Rev. B **51**, 17379 (1995).
[21] J. W. Mintmire and C. T. White, Synth. Met. **77**, 231 (1996).
[22] R. R. Dagastine, D. C. Prieve, and L. R. White, J. Colloid Interface Sci. **231**, 351 (2000).
[23] H. D. Ackler, R. H. French, and Y. M. Chiang, J. Colloid Interface Sci. **179**, 460 (1996).
[24] J. Israelichvili, *Intermolecular and Surface Forces*, 2nd ed. (Academic, New York, 1991).
[25] The nonretarded case applies at small induced-dipole separations when $\omega d/c$ is small and no phase lag develops between the oscillations of the induced dipoles due to a finite speed of light, c.
[26] The single layer formulation can be generalized to any number of layers (Ref. 29) and computations of $A_{1...N}$ from optical properties of each medium is facilitated by open source software at http://sourceforge.net/projects/geckoproj (Ref. 13).
[27] F. Wooten, *Optical Properties of Solids* (Academic, New York, 1972), p. 49.
[28] R. R. Dagastine, D. C. Prieve, and L. R. White, J. Colloid Interface Sci. **249**, 78 (2002).
[29] R. Podgornik, R. H. French, and V. A. Parsegian, J. Chem. Phys. **124**, 044709 (2006).
[30] L. A. Wilen, J. S. Wettlaufer, M. Elbaum, and M. Schick, Phys. Rev. B **52**, 12426 (1995).